Food Anal. Methods (2016) 9:322–331
DOI 10.1007/s12161-015-0198-3

Carbonaceous Materials-12: a Novel Highly Sensitive Graphene Oxide-Based Carbon Electrode: Preparation, Characterization, and Heavy Metal Analysis in Food Samples

Samet Yavuz[1] · Aslı Erkal[1] · İshak Afşin Kariper[2] · Ali Osman Solak[3,4] · Seungwon Jeon[5] · İbrahim Ender Mülazımoğlu[6] · Zafer Üstündağ[1]

Received: 3 March 2015 / Accepted: 4 May 2015 / Published online: 19 May 2015

Abstract Graphene oxide (GO) was covalently attached to glassy carbon (GC) electrode (GC–O–GO) for fabricating nanosensors to determine trace Pb^{2+} and Cd^{2+} using differential pulse anodic stripping voltammetry (DPASV). Surface characterization of the nanofilm-covered electrode was performed via electrochemical cyclic voltammetry (CV), transmission electron microscopy (TEM), atomic force microscopy (AFM), and X-ray photoelectron spectroscopy (XPS) techniques. Surface pKa of the GO covalent attached GC (GC–O–GO) was calculated via CV. Under optimal conditions, a linear response was found for Pb^{2+} and Cd^{2+} in the range from 1×10^{-8} to 1×10^{-12} M. The limit of detections (LODs) of Pb^{2+} and Cd^{2+} were 0.25 pM and 0.28 pM, respectively. The method shows good reproducibility, and stability was successfully applied to measure Pb^{2+} and Cd^{2+} levels in rice, soya, milk, and tap water samples, with good agreement with those obtained by the standard inductively coupled plasma optical emission spectrometry (ICP-OES) method. The method was evaluated by application with the simultaneous determination of the ions in food samples ($n=6$) using the standard addition method. The recoveries of the Pb^{2+} and Cd^{2+} were up to 98 %.

Keywords Differential pulse anodic stripping voltammetry · Graphene oxide modified glassy carbon electrode · Lead and cadmium analysis · Food samples

Introduction

Heavy metal concentration in food samples is very important for human health (Afkhami et al. 2011; Cayir and Coskun 2010; Ieggli et al. 2010). This is the cause of various health problems, such as cardiovascular diseases, kidney failure, cancer, etc. (Kadıoğlu et al. 2010). It is important to accurately determine levels by using various analytical techniques. Techniques such as spectroscopic and electrochemical methods are used for metal analysis (Szymczycha-Madeja and Welna 2013; Üstündağ et al. 2007; Tormen et al. 2011). Electrochemical techniques on modified electrodes are especially very sensitive for metal solutions with very low concentrations (Wei et al. 2012a; Wang et al. 2014; Ensafi 2010).

The scientists have been discussing the impact of environmental exposure to toxic metals on human health especially caused by lead and cadmium for more than 30 years. General evaluation of the toxic influences of Pb and Cd on people living in polluted areas is obviously based on analysis of the amount these toxic elements in urine and blood (Minoia et al. 1990; Hamilton et al. 1994). Not only toxic metals such as Pb and Cd but also some essential metals like Mn, Ca, Fe, Zn, Ni,

✉ İbrahim Ender Mülazımoğlu
iemulazimoglu@konya.edu.tr

✉ Zafer Üstündağ
zustundag@gmail.com

[1] Faculty of Arts and Science, Department of Chemistry, Dumlupinar University, 43100 Kütahya, Turkey

[2] Faculty of Education, Erciyes University, 38039 Kayseri, Turkey

[3] Faculty of Engineering, Chemical Engineering Department, Kyrgyz-Turkish Manas University, Bishkek, Kyrgyzstan

[4] Faculty of Science, Department of Chemistry, Ankara University, 06100 Ankara, Turkey

[5] Department of Chemistry and Institute of Basic Science, Chonnam National University, Gwangju 500-757, South Korea

[6] Faculty of Education, Department of Chemistry, Necmettin Erbakan University, 42090 Konya, Turkey

Co, Cu, Cr, Na and K generally accumulate on noils, hair, and teeth.

Modified electrode has become very attractive for nanosensors in the last two decades (Sanghavi and Srivastava 2011). Differential pulse voltammetry (DPV) (Ensafi 2010), square wave voltammetry (SWV) (Li et al. 2011), amperometry, and electrochemical impedance spectroscopy (EIS) are very highly recommended, sensitive, and low-cost techniques on the modified surfaces for quantitative analysis of various molecules (Ensafi et al. 2011) and metals. A generally modified surface can drastically improve the electrocatalytic properties of electroactive groups, increase the electron transfer rate, and increase the sensitivity of the electrode response (Omidinia et al. 2014). Various methods, such as electrochemical (Baraket et al. 2013), self-assembled monolayers (SAMs) (Güzel et al. 2010), chemical (Üstündağ and Solak 2009), and physical (Gupta et al. 2013) techniques have been reported for the electrochemical quantitative analysis in various environmental and food samples. Most of the transition metals, such as Cu, Cd, Co, Fe, Ni, Zn, etc., and a lot of other metals, such as Sn, As, Sb, Pb, Bi, etc., are analyzed via electrochemical voltammetric methods. In the literature, chemical analysis of heavy metals in food samples by using voltammetry has greatly increased in recent years. Wei et al. studied toxic metal composition in drinking water on AlOOH(boehmite)@SiO_2/Fe_3O_4 porous magnetic microspheres modified glassy carbon (Wei et al. 2011) via square-wave anodic stripping voltammetry (SWASV). They reported that the LOD was calculated as 0.0103 and 0.0156 ng L^{-1} for $Pb^{2+}$and Cd^{2+}, respectively. Abbasi et al. investigated the performance of the Pb^{2+} and Cd^{2+} analysis on 2-mercaptobenzothiazole modified hanging mercury drop electrode via voltammetry (Abbasi et al. 2011). In this paper, linear calibration curves were established in the range of 0.5–70 and 0.2–30 ng mL^{-1}, for Pb^{2+} and Cd^{2+}, respectively, with a detection limit of 0.017 ng mL^{-1} for Pb^{2+} and 0.01 ng mL^{-1} for Cd^{2+}. They used the rice, soya, and sugar as real samples in the article. Illuminati et al. investigated a new method for the determination of Cd^{2+}, Pb^{2+}, and Cu^{2+} in wine (Illuminati et al. 2013). They prepared an epoxy-impregnated graphite electrode. The LOD values were determined as 1.2 and 7.0 ng L^{-1} for Pb^{2+} and Cd^{2+}, respectively. In another study, some trace metals were analyzed in a honey sample on a boron-doped diamond electrode via DPASV (Honório et al. 2014). LOD was calculated as 0.40 and 1.28 ppb for Pb^{2+} and Cd^{2+}, respectively, in the article.

Although a definition for graphenes does not yet exist, graphene has given direction to the scientific world since its first synthesis. The name graphene is already confusing to scientists as graphite oxide and GO. Many researchers describe graphene as consisting of a single atomic sheet of conjugated sp^2 carbon atoms and a 2D single layer of graphite (Goh and Pumera 2010; Loh et al. 2010). The GO has a C:O ratio of 2–3, and the same characteristic properties are observed in graphene. However, GO has functional (such as C=O, –OH, and –COOH) and aromatic groups with different properties compared to graphene. Reduced graphene oxide (rGO) is more aromatic than GO and has the same properties as graphene, which include electrical, thermal, and mechanical properties. Case graphite has well-stacked layers parallel to each other in a three-dimensional crystalline structure. The chemical bonds within the layers are covalent, with the same sp^2 hybridization as other members of the graphene family. Graphite oxide has many layers of GO (Fitzer et al. 1995). Graphene and its derivatives are advantageous to science in a variety of technological areas, such as electronics (Novoselov et al. 2004; Gilje et al. 2007), sensors (Schedin et al. 2007), electromechanics (Bunch et al. 2007), solar cells (Wang et al. 2008), memory devices (Standley et al. 2008), hydrogen storage (Sofo et al. 2007), ultracapacitors (Stoller et al. 2008), field-effect transistors (FET), and biomedical applications (Geim and Novoselov 2007). In recent years, graphene-derivative nanomaterials and nanotubes have garnered much popularity in the field of electroanalytical study. This dramatic interest can be based on the use of electrocatalytically affected GOs (Eng and Pumera 2014). Several electrochemical nanosensors, based on graphene and its derivatives, have been developed for various samples, such as biological (Hasanzadeh et al. 2013) and environmental (Hasanzadeh et al. 2012). The physicochemical properties of GO provide researchers an opportunity for metal detection. The functional groups of GO or binding some molecules on GO provides for detection of heavy metals very easily (Lü et al. 2013). Li et al. (2014) studied Cd^{2+} and Pb^{2+} analysis on electroreduced GO (erGO) modified bismuth-film electrode by SWV. They calculated the LOD as 0.1 μg L^{-1} for Cd^{2+} and 0.05 μg L^{-1} for Pb^{2+}. Shaoo et al. (2013) determined heavy metals on a reduced GO/Bi nanocomposites modified surface by DPV. In the study, LOD of Cd^{2+} and Pb^{2+} were determined as 2.8 and 0.55 μg L^{-1}, respectively. Ouyang et al. (2011) analyzed Zn^{2+}, Cd^{2+}, and Pb^{2+} on the Hg-Bi included carbon nanotube modified GC electrode by SWV. They reported that the LODs for Cd^{2+} and Pb^{2+} were lower than 2 ppm and 0.12 ppb, respectively. In an article, Zhu et al. (2014) studied analysis of Pb^{2+} and Cd^{2+} on a gold nanoparticle–graphene–cysteine composite modified bismuth film electrode via voltammetry. LOD was calculated as 0.10 ppb for Cd^{2+} and 0.05 ppb for Pb^{2+}.

The present work, therefore, aims to apply GO modified GC electrode as a working electrode for the simultaneous measurement of Pb^{2+} and Cd^{2+} concentrations by the DPASV method. The nanostructure was characterized using XPS, TEM, AFM, and electrochemical techniques. The sensitivity of response for the ions and the detection limits was also investigated to show the applicability of the method.

Experimental

All highest purity chemicals were obtained from Merck, Sigma-Aldrich, Fluka, or Riedel de Hean chemical companies. The water was purified in ultrapure water (UPW) by a resistance of 18.3 MΩ (Human Power 1+ purification system, S. Korea). All experiments were performed under a purified Argon gas (99.999 %) atmosphere. All experiments were performed at room temperature (25±1 °C) in the triple electrode system. The reference electrode was an Ag/AgCl/KCl (sat) and Ag/Ag+(0.01 M) in aqueous and non-aqueous media, respectively. Pt wire was used as auxiliary. The GC working electrode was gathered from BAS (Bioanalytical Systems, MF-2012, USA) for electrochemical modification and characterization, such as CV and EIS measurements. The other surface characterization of the nanofilm was performed on a GC-20 (Tokai, Japan) electrode. Carbon electrodes were cleaned with 100 and 50 nm Al_2O_3 suspension (Baikowski Int. Corp., USA) on polishing clothes (Buehler, Lake Bluff, IL, USA) for approximately 5 min and then washed with UPW and acetonitrile (CH_3CN). Polished GC electrodes were sonicated (Ultrasonic Cleaner, SK1200H, China) in UPW and isopropyl alcohol/ CH_3CN (1:1, *v/v*) for approximately 5 min.

Preparation of GO and GC–O–GO

GO were prepared using the method described earlier (Hou et al. 2010). Briefly, the GO was synthesized from natural graphite by a modified Hummers method. To start, graphite powders were oxidized with sulfuric acid. Five grams of graphite oxide was placed in 25 mL of sulfuric acid; then 5 g $K_2S_2O_8$ and 5 g P_2O_5 were added. The mixture was heated at 80 °C for 6 h. Then it was cooled to about 30 °C. The mixture was washed with water and sonicated to remove the residual acid. The product was kept under ambient conditions for 12 h. The pretreated graphite powder was added to cold (0 °C) H_2SO_4 (250 mL). Then $KMnO_4$ (30 g) was inserted into the mixture by stirring at less 20 °C. When the addition was completed, the mixture was kept and stirred at 35 °C for 4 h, and then 500 mL UPW was added. During the dilatation step, the temperature of the oxidation reaction was carried out under 50 °C with an ice bath; 500 mL UPW was added and stirred for 2 h. Following the stirring, 1.5 L UPW and 40 mL %30 H_2O_2 were added. The color of the mixture changed to brilliant yellow and began to bubble. The GO suspension was centrifuged and washed with 0.1 M HCl three times to remove metallic pollution, followed by 1.0 L UPW water.

Two hundred milligram GO was diluted in 25 mL 0.01 M HCl. The bare GC was modified with the GO in the suspension solution under the positive potential for three CV cycles. The modified surface was denoted as GC–O–GO. The electrochemical measurements were acquired with a Gamry Reference 300 electroanalyzer (USA). The proposed structure of the GC–O–GO surface constructed by the electrochemical binding mechanism is shown in Scheme 1.

Characterization of GC–O–GO

CV and EIS characterization was carried out in 1 mM $K_3Fe(CN)_6$+1 mM $K_4Fe(CN)_6$ solution in 0.1 M KCl supporting electrolyte using the electroanalyzer system. The pKa of the GC–O–GO was determined with the redox couple by CV methods. The second redox probe characterization of a modified surface was performed with 1 mM ferrocene in 0.1 M tetrabutylammonium tetrafluoroborate (NBu_4BF_4) in CH_3CN. EIS data of the $Fe(CN)_6^{3-/4-}$ redox couple was measured at 300 kHz to 0.1 Hz at 10 mV wave amplitude with 0.165 V of DC potential.

XPS measurements were performed by using a PHI 5000 Versa Probe (ϕ ULVAC-PHI, Inc., Japan/USA). The modified surface was characterized via an AFM microscopy (NT-MDT atomic force microscopy), with a non-contact mode of resonant

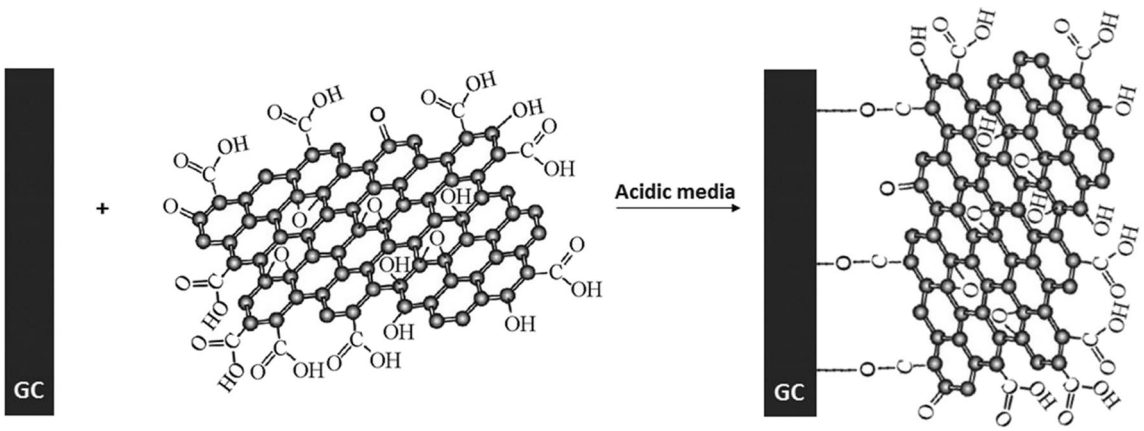

Scheme 1 Schematic diagram of GC–O–GO

freq. 150 kHz force constant 5 N/m. The GO was imaged using a JEOL 2100 HRTEM instrument (JEOL Ltd., Tokyo, Japan).

Determination of Simultaneous Cd^{2+} and Pb^{2+} in Aqueous Media with DPASV

Cd^{2+} and Pb^{2+} ions were adsorbed on the GC–O–GO surface in 0.1 M acetate buffer solution with various pH, accumulation time, and temperature. The optimum condition of the sensor application was calculated via anodic stripping DPV. Optimization of pH, deposition time, and temperature were investigated for the range of 3.5–5.5 pH, 10–50 min, and 20–40 °C, respectively. Before DPASV measurements, Pb^{2+} and Cd^{2+} ions on the modified surface were reduced to metallic forms at −1.0 V for 10 s in 0.1 M acetate buffer solution. A traditional milk sample was 1:1 (*v*/*v*) diluted with UPW. The pH value of the milk sample was adjusted at 4.5 via 0.1 M acetate buffer solution. The tap water sample was taken from our research laboratory in Dumlupinar University without pretreatment before determination; the pH value was adjusted to 4.5 with 0.1 M acetate buffer solution. One gram of the rice and soya seed samples was weighed and powdered with an agate mortar. In a beaker, 15 mL of concentrated HNO_3 was added to the soya and rice powdered samples and was kept overnight. The suspensions were evaporated near to dryness on a magnetic hotplate at about 120 °C for 4 h. The residues were dissolved in 0.5 M HNO_3 and centrifuged to remove particles from the suspension (Rajabi et al. 2014). The pH of the media adjusted at 4.5 via 0.1 M acetate buffer solution. The measurements of the all samples were repeated five times (n=5).

Results and Discussion

Electrode Modification and Characterization

The GO (TEM imaging of the GO is given in Fig. 1a) was electrochemically attached on GC electrode via CV voltammetry. Oxidation voltammogram of GO on GC electrode in 0.01 M HCl is given in Fig. 1b as four cycles. The modification process was completed after the first cycle. The modification of the GO on GC electrode was checked through a second experiment. Under the same conditions, the bare GC electrode was scanned in a positive direction in 0.01 M HCl without GO. The voltammogram is given in Fig. 1c. In an article, during the positive scanning, various functional groups such as –OH, C=O, and –COOH are composed on the GC electrode surface (McCreery and Bard 1991). Behavior of the ferrocene on GC, GC–ox, and GC–O–GO electrodes is shown in Fig. 2a. In the figure, it is explicitly shown that the electron transfer rate of ferrocene on GC–ox is faster than on GC–O–GO. The electrochemical behavior of $Fe(CN)_6^{3-/4-}$ redox couple on GC, GC–ox, and GC–O–GO electrodes in 0.1 M KCl in aqueous media is given in Fig. 2b. GC–O–GO surface shows a higher blocking ability than GC–ox for the $Fe(CN)_6^{3-/4-}$ electron transfer reaction. These two redox probe characterizations show that GO was covalently attached on a GC surface via electrochemical oxidation.

The pH dependence of $Fe(CN)_6^{3-/4-}$ occurred when the pH of the bulk solution changed. Carboxylic acid groups on the modified surfaces have a major effect with the various pH of the buffer solution. The cyclic voltammogram of the redox probe on GC–O–GO is given in Fig. 2c. The electron transfer rate of the redox couple on GC–O–GO was changed with the pH of the media. When the pH of the solution was high enough from the pKa value of the surface, the carboxylic acid groups were charged as negative. The negatively charged GC–O–GO surface significantly decreased the negatively charged $Fe(CN)_6^{3-/4-}$ by repelling them with the electrostatic effect. The cathodic peak current data of the redox couple with various pH on the GC–O–GO surface is given in Fig. 2d. The surface pKa of the GC–O–GO was determined as 3.18±0.30 by Gaussian fitting. In an article, pKa of colloidal GO was determined as 4.3 (Konkena and Vasudevan 2012). The carboxyl and hydroxyl groups involved with a graphene surface behave like carbon nanotubes, which probably have pKa values ranging from 3 to 5 (Tarley et al. 2006).

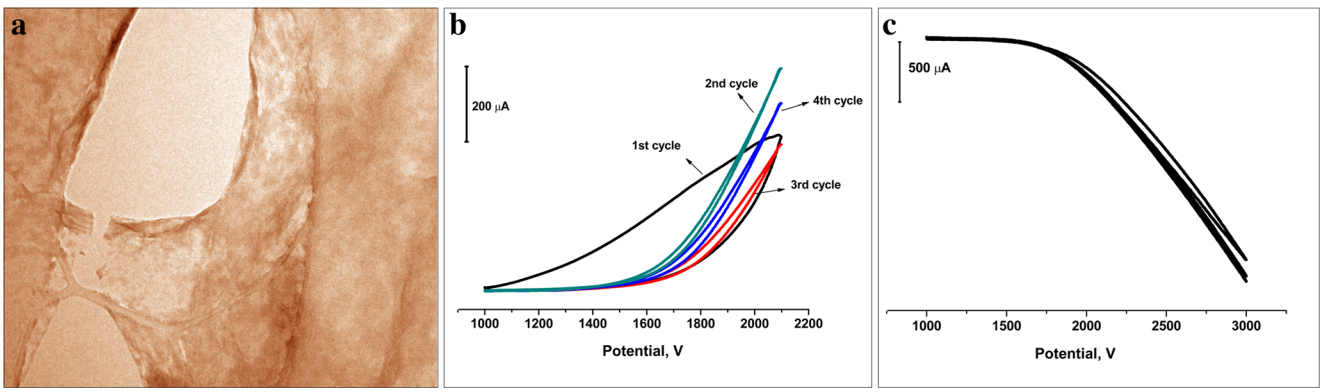

Fig. 1 TEM imaging of the GO (**a**), cyclic voltammograms of presence of GO (**b**), and without GO (**c**) on GC in 0.01 M HCl media. Scan rate is 200 mV s^{-1} vs. $Ag/AgCl_{(sat)}$ reference electrode

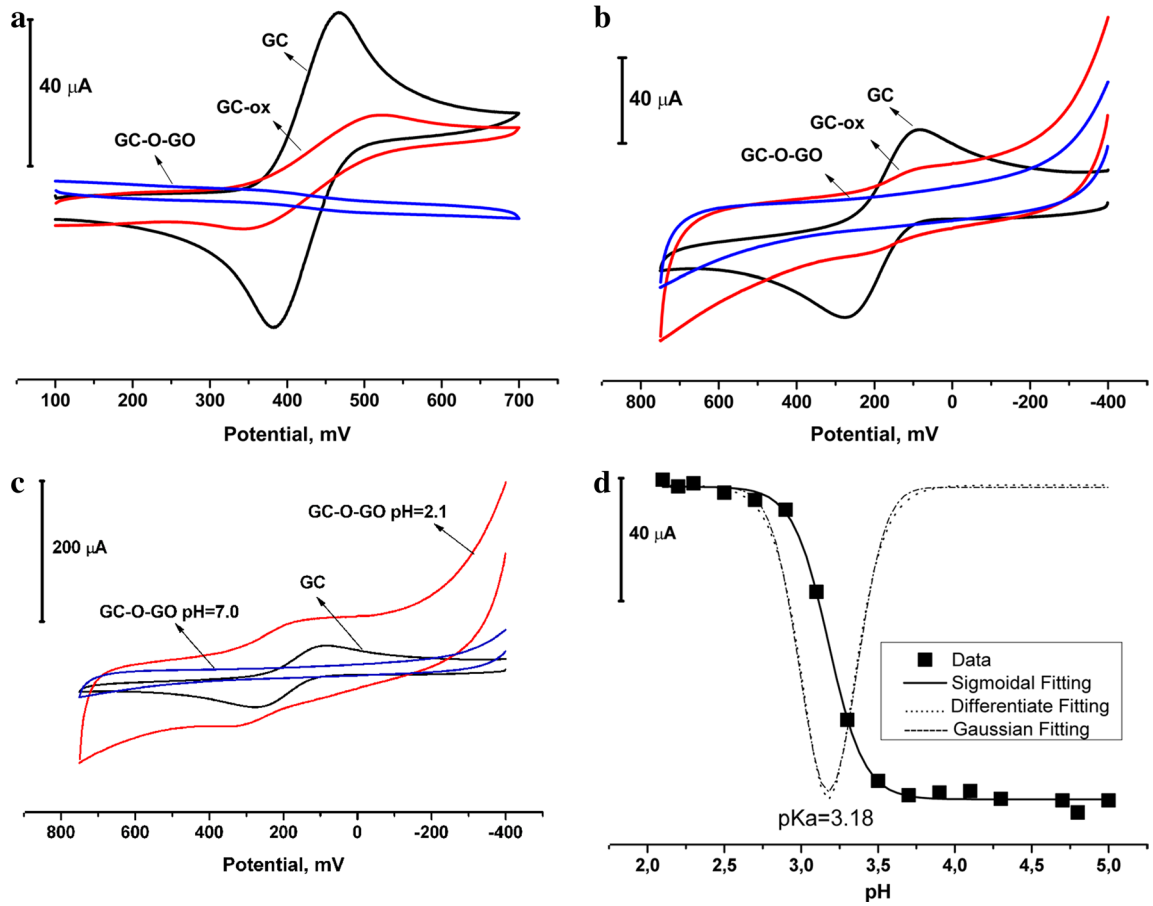

Fig. 2 Cyclic voltammograms of 1 mM ferrocene (**a**) and $Fe(CN)_6^{3-/4-}$ (**b**) on GC, GC–ox, and GC–O–GO; cyclic voltammograms of 1 mM $Fe(CN)_6^{3-/4-}$ on GC and GC–O–GO at pH=7.0 and 2.1 (**c**), scan rate is 200 mVs^{-1} vs. Ag/Ag^{+}(0.01 M) and $Ag/AgCl_{(sat)}$ reference electrode, non-aqueous and aqueous media, respectively; cathodic peak currents versus pH plot of the surfaces in $Fe(CN)_6^{3-/4-}$ redox probe and derivative curve (**d**)

The experimental data of EIS was fitted with a diffusion-affected constant phase element (CPE; Y_o and α value) or Warburg (Z_w)-affected Randles equivalent circuit as shown in Fig. 3a–c. The experimental data was obtained at a 300-kHz–0.1-Hz frequency range using a 1 mM $Fe(CN)_6^{3-/4-}$ redox couple in 0.1 M KCl in aqueous solution by using EIS under 0.165 mV of DC potential. The fitting values are shown in Table 1. The resistance of the solution with supported electrolyte (R_s) was determined to be between 85 and 140 Ω. The charge transfer resistances (R_{ct}) of the redox couple on the GC electrode and GC–ox were nearly 3–4 kΩ. The R_{ct} of redox couple probes on GC–O–GO was fitted as 120 kΩ. The GC–

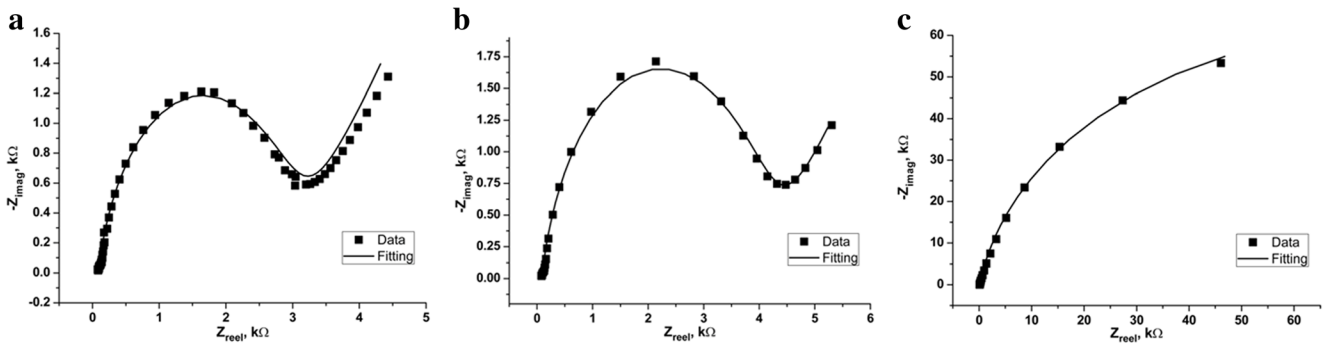

Fig. 3 The Nyquist plots of GC (**a**), GC–ox (**b**), and GC–O–GO (**c**) and their fittings curves

Table 1 Fitting values of Warburg affected CPE circuit for 1 mM $Fe(CN)_6^{3-/4-}$ redox couple on bare GC and GC–ox and GC–O–GO in 0.1 M KCl in aqueous media

Sample	R_s (Ω)	Y_o for CPE ($S.s^{1/2}$)	α for CPE	Z_w (Ω)	R_{ct} (Ω)
GC	85.95±1.20	$(3.01\pm0.02)\times10^{-6}$	0.841±0.010	$(4.800\pm0.001)\times10^{-4}$	$(2.935\pm0.05)\times10^{3}$
GO–ox	85.51±0.01	$(2.974\pm0.116)\times10^{-6}$	0.848±0.004	$(5.812\pm0.044)\times10^{-4}$	$(4.092\pm0.04)\times10^{3}$
GC–O–GO	135.80±0.01	$(8.538\pm0.038)\times10^{-6}$	0.902±0.030	$(5.118\pm0.003)\times10^{-4}$	$(120.3\pm1.2)\times10^{3}$

O–GC surface has exhibited different behavior according to GC electrode and GC–ox.

The formed GC–O–GO was confirmed by XPS measurements, which are effective tools to characterize the presence of C and O elements. The C_{1s} and O_{1s} binding energy spectra of the GC–O–GO surface are given in Fig. 4a, b. The narrow region high-resolution C_{1s} core spectra of GC–O–GO fit as four peaks, which were O–C=O at 288.8 eV, C=O at 287.8 eV, C–O at 286.7 eV, and C–C at 284.9 eV in Fig. 4a (Tu et al. 2014). The O_{1s} spectrum of the modified surface shows peaks at 533.8, 532.5, 531.8, and 530.7 eV, respectively, which could be assigned to C–C=O/O–C=O; C–OH/C–O, –OH (hydroxides), C=O, and other carbon complexes (Fig. 4b).

AFM imaging of the bare GC electrode is given in Fig. 4c. The AFM images of the GO terminated thin film (GC–O–GO) are shown in Fig. 4d. The GC electrode surface has a few aluminum polishing matter-affected pinholes or scratches at the 1–10-nm scale. The imaging of the modified surface has nanometer and micrometer scaled changeable roughness because of horizontal or vertical located GO with a micrometer scale. Some regions of the modified surface are smoother than bare GC electrode surfaces.

Calibration Curves of Cd^{2+} and Pb^{2+} on the GC/GO

Some analysis parameters that affect the simultaneous analysis of the Pb^{2+} and Cd^{2+}, such as the pH factor, deposition time, and deposition temperature, were optimized via DPV. The maximum current of the Pb^{2+} and Cd^{2+} were measured at pH 4.5 (Fig. 5a). The optimum deposition time was determined as achieved at 30 min (Fig. 5b). The incubation temperature of the ions was calculated as 28 °C (Fig. 5c).

Figure 6a shows DPASV responses of concentrations of Cd^{2+} and Pb^{2+} on the GO covalently modified carbon

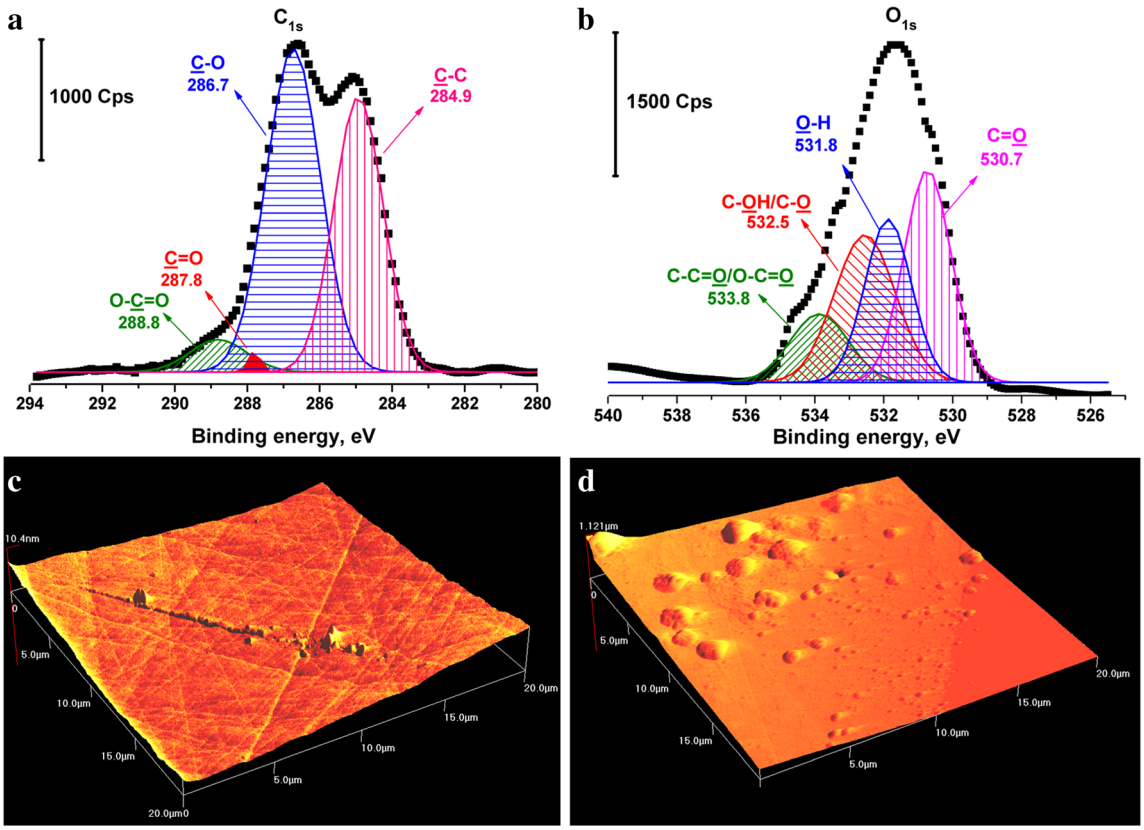

Fig. 4 High-resolution XPS core spectra of GC–O–GC: C_{1s} (**a**) and O_{1s} (**b**); AFM images of bare GC (**c**) and GC–O–GO (**d**)

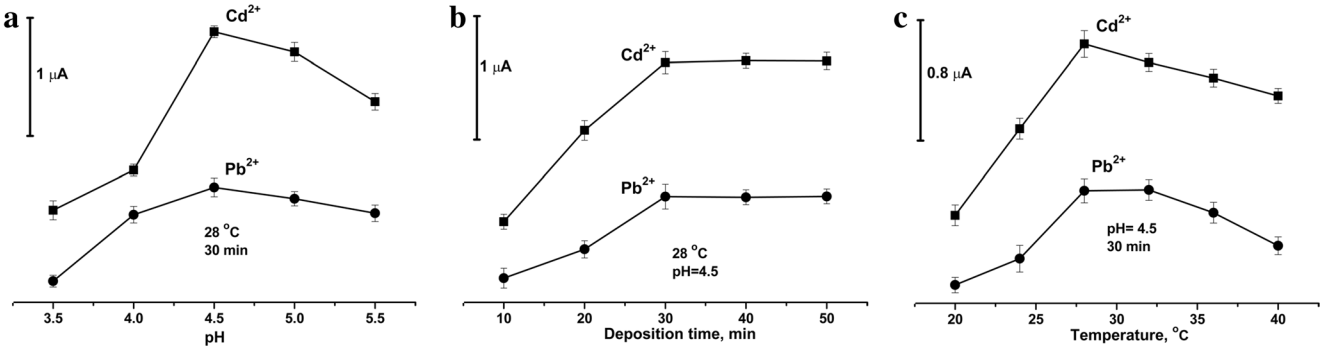

Fig. 5 Optimization, pH at 28 °C for 30 min (**a**), deposition time at 28 °C for pH=4.5 (**b**) and deposition temperature at pH=4.5 for 30 min (**c**) for Pb^{2+} and Cd^{2+}

electrode surface and their Gaussian fits. The determination limits of Cd^{2+} and Pb^{2+} have been tested by DPASV measurements on the GO covalently modified carbon electrode in 0.1 M acetate buffer (pH 4.5) range of 1×10^{-6} M–1×10^{-12} M Cd^{2+} and Pb^{2+}. The electrical signals were observed at −631.2 mV for Cd^{2+} and −329.2 mV for Pb^{2+}, approximately. The signals of the stripping peaks of Cd^{2+} were more intensive than that of Pb^{2+}; the stripping peaks of Cd^{2+} were twofold, according to the stripping peaks of Pb^{2+}. This means the electron transfer of Cd^{2+} ions on the GO surface is faster than that of Pb^{2+} ions. Hence, the GC–O–GO surface features the highest sensitivity and the best stability for trace concentrations of Pb^{2+} and Cd^{2+}. The carboxylate and hydroxyl groups of the GO surface can electrostatically attract Pb^{2+}

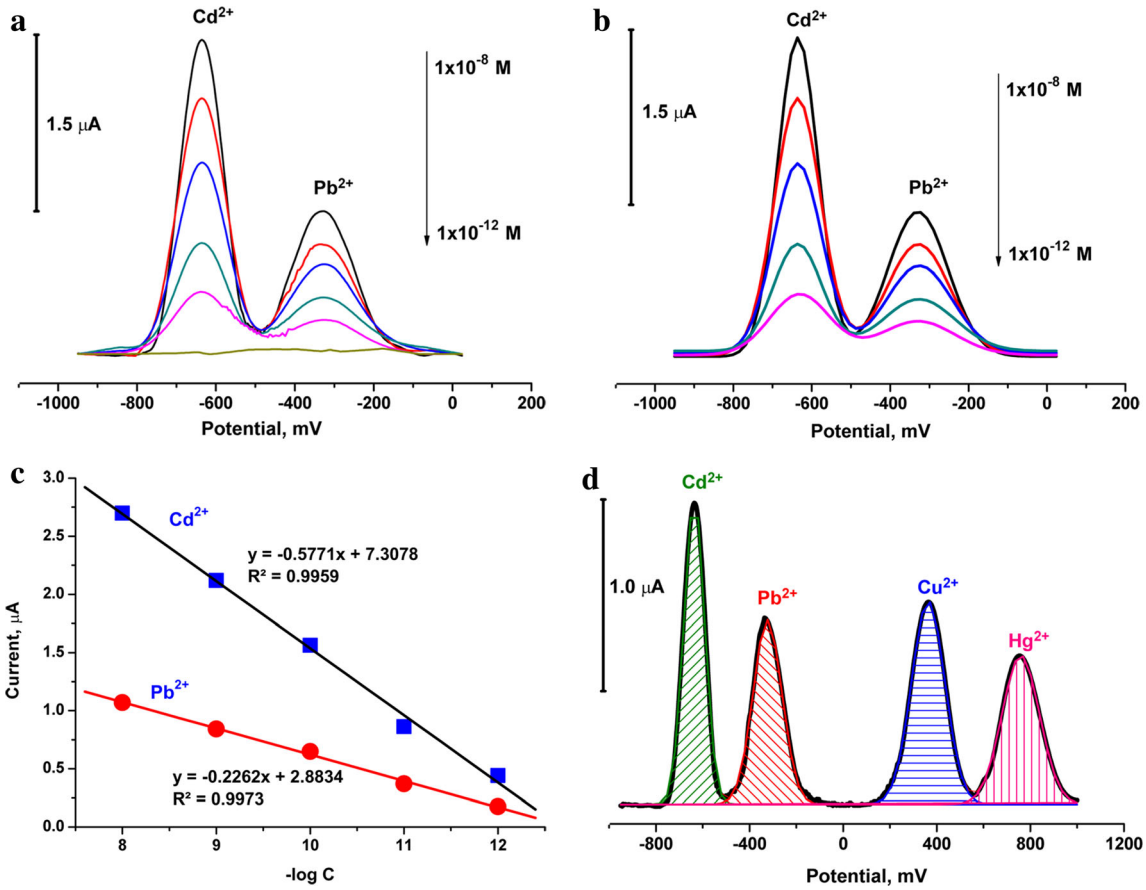

Fig. 6 DPASV calibration voltammograms (**a**) of 1×10^{-8}, 1×10^{-9}, 1×10^{-10}, 1×10^{-11}, and 1×10^{-12} M Cd^{2+} and Pb^{2+} on the GC–O–GO and their Gaussian fittings (**b**); calibration curves of Cd^{2+} and Pb^{2+} on the GC–O–GO (**c**) and DPASV voltammogram for interference effects of the method (**d**) in aqueous media

Table 2 Precision and accuracy results of the methods for intra-day and inter-day

Added Cd^{2+}/Pb^{2+}	Intra-day			Inter-day		
	Found value for Pb^{2+} and Cd^{2+}	Precision % for Pb^{2+} and Cd^{2+}	Accuracy % for Pb^{2+} and Cd^{2+}	Found value for Pb^{2+} and Cd^{2+}	Precision % for Pb^{2+} and Cd^{2+}	Accuracy % for Pb^{2+} and Cd^{2+}
1 nM	1.01±0.02/1.02±0,02	1.98/1.96	1.00/2.00	1.00±0.02/1.02±0.03	2.00/2.94	0.00/2.00
4 nM	4.01±0.03/3.98±0,01	0.75/0.25	0.25/−0.50	3.99±0.01/4.01±0.02	0.25/0.50	−0.25/0.25
7 nM	6.93±0.07/7.03±0.03	1.01/0.43	−1.00/0.43	7.02±0.04/6.97±0.03	0.57/0.43	0.28/−0.43

and Cd^{2+} ions. This means that Pb^{2+} and Cd^{2+} ions also show chemical attraction with oxygen atoms on the GO surface (Wei et al. 2012b).

Figure 6a, b presents calibration voltammograms of different concentrations of Pb^{2+} and Cd^{2+} on the GO covalently modified carbon electrode according to Gaussian data. At the optimal conditions, simultaneous analysis of Cd^{2+} and Pb^{2+} was performed. Also, the analysis of Cd^{2+} and Pb^{2+} ions was performed by changing the concentration of both species. As shown in Fig. 6c, the linear graphs of Pb^{2+} and Cd^{2+} are $y=-0.2262x+2.8834$ ($R^2=0.9973$) and $y=-0.5771x+7.3078$ ($R^2=0.9959$), respectively. The mutual responses of species are practically unaltered with the increase of another species concentration. The detection limits of Cd^{2+} and Pb^{2+} were 2.5×10^{-13} and 2.8×10^{-12} M, respectively. The Cd^{2+} calibration curve slope is especially higher than that of Pb^{2+}. A GC–O–GO electrode surface is more selective for Cd^{2+} than Pb^{2+}. LOD results of the methods are satisfactory as compared to the values given in many articles in the literature.

Three different concentrations of 1.0, 4.0, and 7.0 nM Pb^{2+} and Cd^{2+} in the linear range were analyzed in six independent series on the same day for intra-day precision and six consecutive days for inter-day precision from six measurements of every series. The precision and accuracy results are given in Table 2. The RSD or precision % values varied from 0.25 to 1.98 for intra-day and from 0.25 to 2.94 for inter-day precision. Accuracy of this method was calculated as the percent relative error. Both of the results obtained for intra-day and inter-day accuracy were ≤2.00 %.

Analysis of Food Samples

The applicability of the GC–O–GO electrode for the analysis of food and water samples with a different variety of real samples with different matrix was assessed by its application to the simultaneous determination of the ions in various real samples, including tap water, rice, soya, and milk. The analysis results of the samples are collected in Tables 3. The results

Table 3 Simultaneous determination of Cd^{2+} and Pb^{2+} in real samples ($n=5$)

Samples	Added, nM		Analyte, nM		ICP-OES, nM		Recovery, %	
	Cd^{2+}	Pb^{2+}	Cd^{2+}	Pb^{2+}	Cd^{2+}	Pb^{2+}	Cd^{2+}	Pb^{2+}
Rice	–	–	1.37±0.05	0.96±0.05	1.41±0.07	1.07±0.06	–	–
	1.0	1.0	2.36±0.06	2.04±0.08	2.49±0.08	2.02±0.05	99.6	104.1
	3.0	3.0	4.43±0.07	3.92±0.09	4.50±0.07	4.05±0.07	101.4	99.0
	5.0	5.0	6.31±0.08	6.01±0.08	6.35±0.06	5.96±0.07	99.1	100.8
Tap water	–	–	1.14±0.06	3.48±0.08	1.10±0.09	3.52±0.08	–	–
	1.0	1.0	2.10±0.08	4.53±0.10	2.13±0.05	4.61±0.09	98.1	101.1
	3.0	3.0	4.08±0.07	6.39±0.07	3.98±0.08	6.37±0.06	98.6	98.6
	5.0	5.0	6.07±0.09	8.46±0.08	6.18±0.07	8.48±0.08	98.9	99.8
Soya	–	–	2.57±0.07	3.36±0.07	2.66±0.07	3.41±0.06	–	–
	1.0	1.0	3.54±0.07	4.41±0.05	3.59±0.07	4.45±0.08	99.2	101.1
	3.0	3.0	5.51±0.08	6.38±0.07	5.61±0.08	6.52±0.07	98.9	100.3
	5.0	5.0	7.61±0.06	8.32±0.08	7.70±0.06	8.39±0.05	100.5	99.5
Milk	–	–	1.98±0.08	1.13±0.06	2.06±0.12	1.08±0.06	–	–
	1.0	1.0	3.06±0.10	2.11±0.07	3.01±0.08	2.14±0.05	102.7	99.1
	3.0	3.0	4.93±0.07	4.08±0.06	5.13±0.08	4.02±0.06	99.0	98.8
	5.0	5.0	7.04±0.08	6.12±0.06	7.01±0.05	6.17±0.07	100.9	99.8

obtained by the DPASV method show a good agreement with those obtained by ICP-OES. The results confirm the applicability of this method for precise and accurate determination of the Cd^{2+} and Pb^{2+} ions in a wide variety of some real samples with different complex matrices. The recovery values of Cd^{2+} and Pb^{2+} in real samples (n=5) are shown in Table 2. The recoveries of the Cd^{2+} and Pb^{2+} were up to 98 %, so analytical recovery was obtained for all species and in the real samples.

Interference Responses of Pb^{2+} and Cd^{2+} Presence in Cu^{2+} and Hg^{2+}

Figure 6d presents DPASV responses of Pb^{2+} and Cd^{2+} in the presence of Cu^{2+} and Hg^{2+} on a GC–O–GO electrode surface. It is well known that matrix affects the ion-selective electrode response. Given strong signals in electrochemical methods, Cu^{2+} and Hg^{2+} metals can affect the response of the electrode (Okcu et al. 2005). We select Cu^{2+} and Hg^{2+}, consciously, because signals of Cu^{2+} and Hg^{2+} are very good. The testing of the matrix effect provides our method a confidence for the matrix effect of Cu^{2+} and Hg^{2+}. The peak current of Pb^{2+} and Cd^{2+} did not affect the equimolar range. The peak current responses of the ions were reduced by about 2 % by the presence of 100-fold excess of Cu^{2+} and Hg^{2+} ions.

Conclusion

The GO was synthesized via the electrochemical exfoliation method as described in the literature. The GO covalently modified on the carbon electrode surface. This prepared electrode was characterized by using TEM, AFM, and XPS. The modified electrode was electrochemically characterized with CV and EIS techniques, assisted with ferrocene and $Fe(CN)_6^{3-/4-}$ redox couples. The proposed method, using GO covalently modified to a glassy carbon surface, is proven to be efficient, sensitive, and rapid and can be used for Pb^{2+} and Cd^{2+} in food samples such as tap water, soya, milk, and rice. Simultaneous determination of Pb^{2+} and Cd^{2+} ions by DPASV is one of the most important advantages of the proposed method, which has been applied on food samples. Effects of this procedure were investigated for electrochemical parameters such as calibration curves and matrix effect. The detection limits of Pb^{2+} and Cd^{2+} were very low. The GO covalently modified carbon electrode surface shows very ultrasensitive response for these cations. The synergistic effect of the GO materials was obtained for Pb^{2+} and Cd^{2+} detection with improved sensitivity and reproducibility.

Acknowledgments We would like to thank the Research Foundation of Necmettin Erbakan University, Konya-Turkey, (BAP-131210012) for the financial support of this work.

Compliance with Ethical Standards

Conflict of Interest Samet Yavuz, Asli Erkal, İshak Afşin Kariper, Ali Osman Solak, Seungwon Jeon, İbrahim Ender Mülazımoğlu, and Zafer Üstündağ have received research grants from Research Foundation of Dumlupınar University (Kütahya, Turkey) and Research Foundation of Necmettin Erbakan University (Konya, Turkey).

Human or Animal Subjects This article does not contain any studies with human or animal subjects.

References

Abbasi S, Khodarahmiyan K, Abbasi F (2011) Food Chem 128:254–257
Afkhami A, Saber-Tehrani M, Bagheri H, Madrakian T (2011) Microchim Acta 172:125
Baraket A, Lee M, Zine N, Sigaud M, Yaakoubi N, Trivella MG, Zabala M, Bausells J, Jaffrezic-Renault NN, Errachid A (2013) Sensors Actuators B Chem 189:165
Bunch JS, van der Zande AM, Verbridge SS, Frank IW, Tanenbaum DM, Parpia JM, Craighead HG, McEuen PL (2007) Science 315:490
Cayir A, Coskun M (2010) The heavy metal content of wild edible mushroom samples collected in Canakkale Province Turkey. Biol Trace Elem Res 134:212
Eng AYS, Pumera M (2014) Electrochem Commun 43:87
Ensafi AA (2010) J Electroanal Chem 640:75
Ensafi AA, Dadkhah M, Karimi-Maleh H (2011) Colloids Surf, B 84:148
Fitzer E, Kochling K-H, Boehm HP, Marsh H (1995) Pure Appl Chem 67:473
Geim AK, Novoselov KS (2007) Nat Mater 6:183
Gilje S, Han S, Wang KL, Kaner RB (2007) Nano Lett 7:3394
Goh MS, Pumera M (2010) Anal Chem 82:8367
Gupta VK, Yola ML, Qureshi MS, Solak AO, Atar N, Üstündağ Z (2013) Sensors Actuators B Chem 188:1201
Güzel R, Üstündağ Z, Ekşi H, Keskin S, Taner B, Durgun ZG, Isbir-Turan AA, Solak AO (2010) J Colloid Interface Sci 351:35
Hamilton EI, Sabbioni E, Van der Venne MT (1994) Sci Total Environ 158:165
Hasanzadeh M, Shadjou N, Saghatforoush L, Mehdizadeh R, Sanati S (2012) Catal Commun 19:10
Hasanzadeh M, Shadjou N, Omidinia E (2013) J Neurosci Methods 219:52
Honório GG, Azevedo GC, Matos MAC, de Oliveira MAL, Matos RC (2014) Food Control 36:42
Hou SF, Su SJ, Kasner ML, Shah P, Patel K, Madarang CJ (2010) Chem Phys Lett 501:68
Ieggli CVS, Bohrer D, Nascimento PC, de Carvalho LM, Garcia SC (2010) Talanta 80:1282
Illuminati S, Annibaldi A, Truzzi C, Finale C, Scarponi G (2013) Electrochim Acta 104:148
Kadıoğlu YK, Üstündağ Z, Solak AO, Karabıyıkoğlu G (2010) Spectrosc Lett 43:247
Konkena B, Vasudevan S (2012) J Phys Chem Lett 3:867
Li H, Li J, Yang Z, Xu Q, Hou C, Peng J, Hu X (2011) J Hazard Mater 191:26
Li Z, Chen L, He F, Bu L, Qin X, Xie Q, Yao S, Tu X, Luo X, Luo S (2014) Talanta 122:285
Loh KP, Bao Q, Ang PK, Yang J (2010) J Mater Chem 20:2277
Lü MJ, Li J, Yang XY, Zhang CA, Yang J, Hu H, Wang XB (2013) Chin Sci Bull 58:2698
McCreery RL, Bard AJ (ed) (1991) Electroanal. Chem., Vol. 17M. Dekker, New York 221

Minoia C, Sabbioni E, Apostoli P, Pietra R, Pozzoli L, Gallorini M, Nicolaou G, Alessio L, Capodaglio E (1990) Sci Total Environ 95: 89
Novoselov KS, Geim AK, Morozov SV, Jiang D, Zhang Y, Dubonos SV, Grigorieva IV, Firsov AA (2004) Science 306:666
Okcu F, Ertas FN, Gokcel HI, Tural H (2005) Turk J Chem 29:355
Omidinia E, Shadjou N, Hasanzadeh M (2014) Mater Sci Eng C 42:368
Ouyang R, Zhu Z, Tatum CE, Chambers JQ, Xue ZL (2011) J Electroanal Chem 656:78
Rajabi M, Mohammadi B, Asghari A, Barfi B, Behzad M (2014) J Ind Eng Chem 20:3737
Sahoo PK, Panigrahy B, Sahoo S, Satpati AK, Li D, Bahadur D (2013) Biosens Bioelectron 43:293
Sanghavi BJ, Srivastava AK (2011) Anal Chim Acta 706:246
Schedin F, Geim AK, Morozov SV, Hill EW, Blake P, Katsnelson MI, Novoselov KS (2007) Nat Mater 6:652
Sofo JO, Chaudhari AS, Barber Phys GD (2007) Matter Mater Phys 75: 153401
Standley B, Bao W, Zhang H, Bruck J, Lau CN, Bockrath M (2008) Nano Lett 8:3345
Stoller MD, Park S, Zhu Y, An J, Ruoff RS (2008) Nano Lett 8:3498
Szymczycha-Madeja A, Welna M (2013) Food Chem 141:3466
Tarley T, Barbosa CR, Gava Segatelli AF, CostaFigueiredo M, Luccas EO, Anal PJ (2006) At Spectrosc 21:1305
Tormen L, Torres DP, Dittert IM, Araújo RGO, Frescura VLA, Curtius AJ (2011) J Food Compos Anal 24:95
Tu Q, Pang L, Chen Y, Zhang Y, Zhang R, Lu B, Wang J (2014) Analyst 139:105
Üstündağ Z, Solak AO (2009) Electrochim Acta 54:6426
Üstündağ Z, Üstündağ İ, Kadıoğlu YK (2007) Appl Radiat Isot 65:809
Wang X, Zhi LJ, Mullen K (2008) Nano Lett 8:323
Wang Z, Wang H, Zhang Z, Liu G (2014) Sensors Actuators B Chem 199:7
Wei Y, Yang R, Zhang Y-X, Wang L, Liu J-H, Huang X-J (2011) Chem Commun 47:11062
Wei Y, Yang R, Yu X-Y, Wang L, Liu J-H, Huang X-J (2012a) Analyst 137:2183
Wei Y, Gao C, Meng FL, Li HH, Wang L, Liu JH, Huang XJ (2012b) J Phys Chem C 116:1034
Zhu L, Xu L, Huang B, Jia N, Tan L, Yao S (2014) Electrochim Acta 115:471